# Low-Complexity Neural Wind Noise Reduction for Audio Recordings

Hesam Eftekhari<sup>1</sup>, Srikanth Raj Chetupalli<sup>2</sup>, Shrishti Saha Shetu<sup>2</sup>, Emanuël A. P. Habets<sup>2</sup>, and Oliver Thiergart<sup>2</sup>

## **Abstract**

Wind noise significantly degrades the quality of outdoor audio recordings, yet remains difficult to suppress in real-time on resource-constrained devices. In this work, we propose a low-complexity single-channel deep neural network that leverages the spectral characteristics of wind noise. Experimental results show that our method achieves performance comparable to the state-of-the-art low-complexity ULCNet model. The proposed model, with only 249K parameters and roughly 73 MHz of computational power, is suitable for embedded and mobile audio applications.

## 1 Introduction

A microphone captures a range of acoustic sources present in the scene. In an outdoor setting, it may also pick up noise induced by the wind flowing past it. Devices such as mobile phones, action cameras, wearables, and hearables frequently encounter wind noise. The turbulent nature of wind flow results in a high-amplitude signal at low frequencies, leading to undesirable distortions in the recorded signal. Hence, effective wind noise reduction (WNR) has become essential to modern consumer audio devices. The increasing adoption of wearables and hearables further amplifies the demand for low-complexity WNR solutions. Although the WNR task resembles speech enhancement (SE), it differs in its objective: the target signal consists of all sound sources, excluding the wind noise component.

Several single-channel approaches [1–8] and multichannel methods [9–11] utilizing traditional signal processing and deep neural network (DNN)-based techniques have been proposed. Earlier approaches used techniques such as adaptive post-filtering in the time domain [1] and methods derived from artificial bandwidth extension [2]. Other approaches [3, 4] concentrated on the estimation of the noise power spectral density (PSD), which is used to obtain spectral gains for WNR. Wind noise exhibits distinct statistical properties in comparison to other acoustic signals, which are leveraged for the PSD estimation. In this context, multi-microphone approaches [9–11], which exploit the spatial characteristics of the received wind noise, have proven to be successful.

In the deep learning context, a bi-directional long short-term memory (LSTM)-based approach was first proposed in [5]. In [6], the authors investigated the estimation of separate masks for the wind and desired signal components, followed by soft masking based on the auditory masking properties. More recent studies [7, 8] employed

a U-Net-based architecture [12] composed of 2D convolutional layers. However, these DNN-based models are not designed for frame-by-frame processing and do not meet the memory and computational complexity constraints of embedded hardware. On the other hand, the SE literature includes several methods that satisfy such design requirements (e.g., [13]); however, these approaches are typically optimized for speech-only scenarios and often suppress music and other non-speech acoustic sources.

In this work, we focus on low-complexity singlechannel WNR techniques for real-time applications on embedded platforms using DNNs. We aim to directly estimate the desired signal by computing a mask, referred to here as the wind rejection approach. Since the desired signal in WNR includes all acoustic sources except wind noise. we also investigate a wind extraction approach, where the DNN estimates a mask for the wind noise itself, which is then removed from the microphone signal to obtain the desired signal. Wind noise is generally concentrated in lowfrequency regions with negligible presence in frequencies above 4 kHz. Motivated by this observation, we propose a dual encoder architecture that emphasizes low-frequency bands while focusing less on higher frequency bands. This design is integrated into the low-complexity ULCNet architecture originally proposed for SE task [13]. Experimental results using speech and music sources validate the effectiveness of the proposed approach for WNR across varied acoustic scenes.

## 2 Problem Formulation

Consider a recording scenario where a single microphone captures an acoustic scene comprising arbitrary sound sources and wind noise. The signal model is expressed

$$\mathbf{x}[n] = \mathbf{s}[n] + \sum_{j=1}^{I_b} \mathbf{b}_j[n] + \mathbf{w}[n], \tag{1}$$

where  $\mathbf{x}[n]$  denotes the recorded microphone signal at discrete time index n, composed of the desired signal  $\mathbf{d}[n]$  and additive wind noise  $\mathbf{w}[n]$ . The desired signal  $\mathbf{d}[n]$  may consist of speech components  $\mathbf{s}[n]$  and  $I_b$  non-speech components  $b_j[n]$ , representing music, ambient noise, or other acoustic sources.

In conventional DNN-based SE approaches [13, 14], a DNN  $\mathscr{F}_{\theta}$  is trained to estimate the clean speech signal  $\widehat{\mathbf{s}}[n]$  from the observed noisy signal  $\mathbf{x}[n]$  using mapping, masking, or deep filtering methods [15]. This formulation does not account for the presence of other non-speech components  $\sum_{j=1}^{I_b} \mathbf{b}_j[n]$ . In this work, we define wind noise as the undesired signal, while treating all other signal components comprising speech or non-speech sound sources as

<sup>&</sup>lt;sup>1</sup> Fraunhofer IIS, Am Wolfsmantel 33, 91058 Erlangen, Germany

<sup>&</sup>lt;sup>2</sup> International Audio Laboratories Erlangen\*, Am Wolfsmantel 33, 91058 Erlangen, Germany Emails: {hesam.eftekhari, srikanth.chetupalli, shrishti.saha.shetu, emanuel.habets, oliver.thiergart}@iis.fraunhofer.de

<sup>\*</sup>A joint institution of Fraunhofer IIS and Friedrich-Alexander-Universität Erlangen-Nürnberg (FAU), Germany.

The authors thank the Erlangen Regional Computing Center (RRZE) for providing compute resources and technical support.

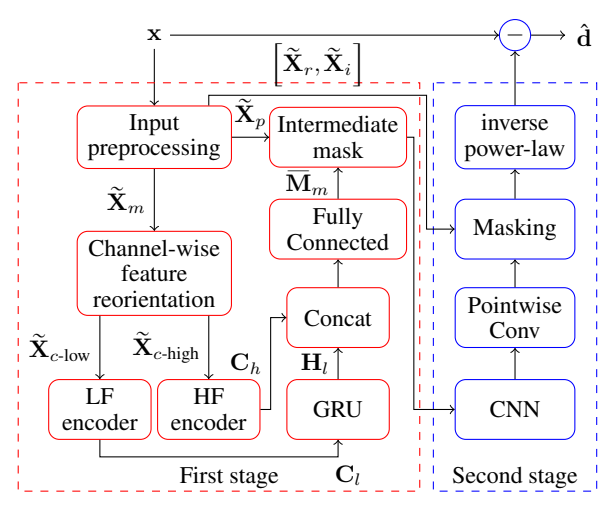


**Figure 1:** The proposed *WindNetLite* model.

desired, i.e., given the noisy signal x[n], the goal in WNR is to estimate the desired signal d[n].

We formulate the wind noise reduction (WNR) problem using two distinct paradigms: wind rejection and wind extraction. In wind rejection, a DNN denoted as  $\mathscr{F}_{rej}$  directly estimates the desired signal,

$$\widehat{\mathbf{d}}[n] = \mathscr{F}_{\text{rej}}(\mathbf{x}[n]).$$
 (2)

However, this approach, especially when combined with masking-based desired signal reconstruction method, often results in signal distortions, particularly in low signal-to-noise ratio (SNR) scenarios where  $\mathbb{E}\left[\|\mathbf{d}[n]\|^2\right] \ll \mathbb{E}\left[\|\mathbf{w}[n]\|^2\right]$  [14, 16]. Therefore, we alternatively investigate a two-stage approach, referred to as *wind extraction*. In the first stage, a DNN, denoted by  $\mathscr{F}_{\text{ext}}$ , estimates the wind noise component

$$\widehat{\mathbf{w}}[n] = \mathscr{F}_{\text{ext}}(\mathbf{x}[n]). \tag{3}$$

Subsequently, the desired signal is recovered using traditional signal processing methods such as post-filtering [1], or direct subtraction [17] as

$$\widehat{\mathbf{d}}[n] = \mathbf{x}[n] - \widehat{\mathbf{w}}[n]. \tag{4}$$

# 3 Proposed Method

In our work, we consider a real-time audio application scenario that requires causal and low-complexity DNN processing. To this end, we adopt the ULCNet-based model architecture [13], originally proposed for noise reduction and shown to be effective in related tasks, such as acoustic echo cancellation and dereverberation [18–20]. ULCNet uses a two-stage process of first estimating a real-valued magnitude mask and then refining it to a phase-enhanced complex mask. We modify this architecture by adding two parallel encoder blocks focusing on low and high frequency regions, respectively, to extract separate intermediate features by exploiting wind noise characteristics. The resulting architecture, referred to as *WindNetLite*, is shown in Fig. 1. In the following, we describe the *WindNetLite* architecture in detail.

## 3.1 DNN Processing

In our architecture, the input preprocessing block first transforms the time-domain signal  $\mathbf{x}[n]$  to short-time

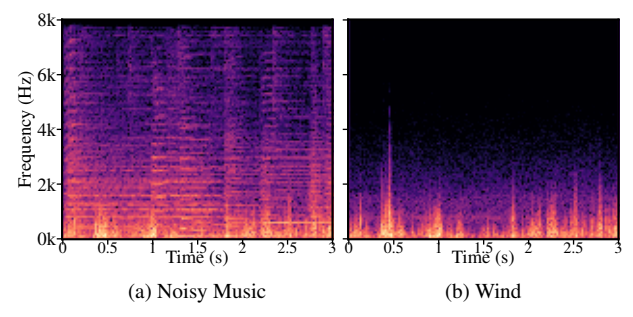


**Figure 2:** (a) A Jazz music signal, corrupted by strong (b) wind noise, limited to the 2-3 kHz frequency range.

Fourier transform (STFT) domain X and then into a power-law compressed representation  $\tilde{X}$ , and extracts magnitude and phase features, as described in [13],

$$\widetilde{\mathbf{X}} = \operatorname{sign}(\Re(\mathbf{X}))|\Re(\mathbf{X})|^{\alpha} + j \cdot \operatorname{sign}(\Im(\mathbf{X}))|\Im(\mathbf{X})|^{\alpha}, \quad (5)$$

$$\widetilde{\mathbf{X}}_{m} = \sqrt{\widetilde{\mathbf{X}}_{r}^{2} + \widetilde{\mathbf{X}}_{i}^{2}}, \quad \widetilde{\mathbf{X}}_{p} = \arctan\left(\frac{\widetilde{\mathbf{X}}_{i}}{\widetilde{\mathbf{X}}_{r}}\right).$$
 (6)

Here, j represents  $\sqrt{-1}$ ,  $\alpha \in [0,1]$  denotes the power-law compression factor, and the sign operator ensures the original sign of the real and imaginary parts is preserved in  $\widetilde{\mathbf{X}}_r$  and  $\widetilde{\mathbf{X}}_i$ . The magnitude feature  $\widetilde{\mathbf{X}}_m \in \mathbb{R}^{B \times T \times F}$  is further reoriented along the channel dimension to reduce the frequency dimension, which aids in reducing the computational cost of convolutional operations [13]. The reoriented channel-wise representation is  $\widetilde{\mathbf{X}}_c \in \mathbb{R}^{B \times T \times L \times N}$ , and considering only the frequency axis, it is defined as:

$$\widetilde{\mathbf{X}}_c = \operatorname{stack}\left(\left\{\widetilde{\mathbf{X}}_m[\dots, i \cdot \widetilde{L} : i \cdot \widetilde{L} + L]\right\}_{i=0}^{N-1}\right),$$
 (7)

where L is the sub-band length, N is the total number of sub-bands, r is the overlap ratio, and  $\widetilde{L} \triangleq L(1-r)$ .

Wind, as illustrated in Fig. 2(b), typically exhibits high energy in the low-frequency range and negligible energy at frequencies higher than 4 kHz. Motivated by this, we propose a dual-encoder architecture with separate encoders for low- and high-frequency regions. The magnitude features  $\mathbf{X}_c$  are first split into low- and high-frequency components, where  $\widetilde{\mathbf{X}}_{c\text{-low}}$  contains the first 5 sub-bands, and  $\widetilde{\mathbf{X}}_{c\text{-high}}$ contains the remaining sub-bands. These components are processed in parallel by two encoder blocks, termed the LF encoder and HF encoder, each consisting of convolutional layers followed by batch normalization and ReLU activation. This design allows the LF encoder to be parameterized with higher complexity, as wind noise is more concentrated in the lower sub-bands, while the HF encoder uses relatively fewer parameters. Both encoders employ a flatten layer to reshape frequency and channel axes into one-dimensional vectors. The output features of the lowand high-frequency encoder modules LF encoder and HF encoder are denoted as  $C_l$  and  $C_h$  respectively. Moreover,  $C_l$  is further processed using a temporal GRU layer. Subsequently, the outputs are concatenated and passed to a fully connected layer with Sigmoid activation to estimate the intermediate real magnitude mask  $\mathbf{M}_m$ ,

$$[\mathbf{H}_{l}, \mathbf{C}_{h}] = [\mathrm{GRU}_{l}(\mathbf{C}_{l}), \mathbf{C}_{h}]$$

$$\overline{\mathbf{M}}_{m} = \mathbf{W}[\mathbf{H}_{l}, \mathbf{C}_{h}] + \mathbf{b},$$
(8)

where W and b represent the learnable weight matrix and bias vector of the fully-connected (linear) layer, respectively. The mask  $\overline{M}_m$  is used to compute intermediate

complex features as described in [13],

$$\widetilde{\mathbf{Y}}_r = \overline{\mathbf{M}}_m \cdot \cos\left(\widetilde{\mathbf{X}}_p\right) \text{ and } \widetilde{\mathbf{Y}}_i = \overline{\mathbf{M}}_m \cdot \sin\left(\widetilde{\mathbf{X}}_p\right). \tag{9}$$

These intermediate features  $\widetilde{\mathbf{Y}}_r$  and  $\widetilde{\mathbf{Y}}_i$  are then concatenated along the channel dimension and passed through a lightweight CNN architecture to estimate a complex mask  $\mathbf{M}$ . The mask is used to reconstruct the power-law compressed estimate of either the desired clean signal  $\widetilde{\mathbf{D}}$  (for wind rejection) or the wind component  $\widetilde{\mathbf{W}}$  (for wind extraction) as follows,

$$\widetilde{\mathbf{D}}$$
 or  $\widetilde{\mathbf{W}} = \widetilde{\mathbf{X}}_m \cdot \mathbf{M}_m \cdot e^{j(\widetilde{\mathbf{X}}_p + \mathbf{M}_p)}$ , (10)

where  $\mathbf{M}_m$  and  $\mathbf{M}_p$  denote the magnitude and phase components of the complex-valued mask  $\mathbf{M}$ , and  $\widetilde{\mathbf{X}}_m$  and  $\widetilde{\mathbf{X}}_p$  are as defined in (6). Finally, after applying power-law decompression using Eq. 5 with a decompression factor  $\beta = \frac{1}{\alpha}$ , followed by inverse STFT, we obtain the estimated time-domain desired signal  $\hat{\mathbf{d}}[n]$  or wind noise  $\hat{\mathbf{w}}[n]$ .

## 4 Experimental Setup

## 4.1 Model Configuration and Baseline

The architecture follows ULCNet[13]-WindNetLite: based convolutional recurrent network design with parallel encoder blocks. The channel-wise feature reorientation operates with L = 40 and an overlap factor of r = 0.4, resulting in N = 10 sub-bands. The input features to both the low-frequency (LF) and high-frequency (HF) encoders have a shape of (B, T, 40, 5). The LF encoder consists of four convolutional layers with {32,64,96,128} filters. Since the higher frequency range does not require full resolution, an average pooling layer with a pool size and stride of (1,2) is applied to the HF input before encoding. The HF encoder comprises three convolutional layers with {8, 16, 64} filters. All convolutions are performed with a kernel size of (1,3) and a stride of (1,2), except for the first layer, which uses a stride of (1,1). The extracted features are subsequently processed using point-wise convolution layers, with 32 filters for LF and 16 filters for HF, to produce the final convolutional features:  $\mathbf{C}_l \in \mathbb{R}^{B \times T \times 5 \times 32}$  and  $\mathbf{C}_h \in \mathbb{R}^{B \times T \times 5 \times 16}$ , respectively. The LF feature  $\mathbf{C}_l$  is further processed through a temporal GRU block with 128 units, yielding  $\mathbf{H}_l \in \mathbb{R}^{B \times T \times 128}$ . These features are then concatenated and passed through a fully connected layer with 257 output units. In the second stage, the CNN consists of 2 convolutional layers with 32 filters each, followed by a point-wise convolution layer, which outputs the final complex mask.

**WindNet:** As the baseline, we adapted the ULCNet model, which we refer to as *WindNet*. In this work, we remove the bidirectional frequency GRU layer and reduce the number of temporal GRU layers in each sub-band from 2 to 1. These modifications are intended to provide a baseline model, *WindNet*, with complexity comparable to the proposed *WindNetLite*.

### 4.2 Training and Test Datasets

We trained the proposed *WindNet* and *WindNetLite* in both the rejection and extraction modes. To compose the training and test datasets, we recorded real wind noise in an outdoor environment using 20 different microphones, corresponding to a total duration of 10 hours. For both training

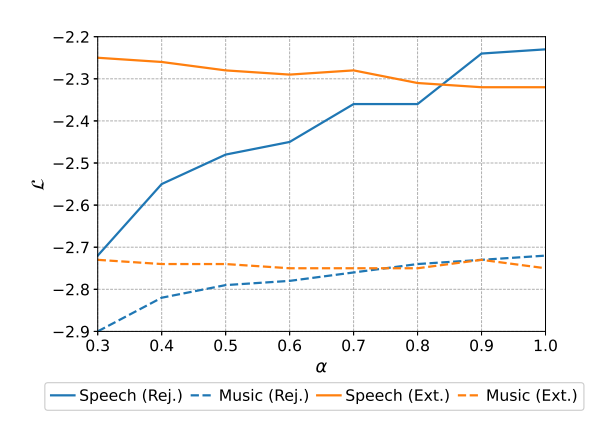


**Figure 3:** Leakage  $\mathscr{L}$  versus Power-law factor  $\alpha$  for speech and instrumental music for extraction and rejection modes.

and validation datasets, we mixed the recorded wind noise with samples from the AudioSet dataset [21] at signal-to-noise ratio (SNR) levels ranging from -20 to 20 dB. AudioSet includes a diverse range of audio categories such as speech, music, and background noises (e.g., roadside traffic, barking, and chirping). The signals from the 'wind' category in AudioSet are excluded from the dataset composition, to prevent data leakage. The resulting training dataset had a total duration of approximately 200 hours.

We created two test sets, each representative of a distinct target signal type commonly encountered in audio recording applications: speech and instrumental music. For the speech test set, the desired signals were taken from the VCTK Voice Bank corpus [22], while the instrumental music samples were drawn from the MUSDB18 corpus [23]. These clean signals were mixed with previously unseen recorded wind noise at SNR levels randomly sampled from the set  $\{-20, dB, -10, dB, 0, dB, 10, dB, 20, dB\}$ . Each test set consisted of 200 samples with a 10 s duration per sample.

#### 4.3 Training Details

We used an STFT with an FFT length of 512, and a Hann window length of 32 ms, with 50% overlap between successive frames, which resulted in 257 frequency bins at 16kHz sampling rate. The MSE computed between the ground truth signal STFT and its estimate computed by the DNN was used as the loss function, as is done in [13] for noise reduction. The Adam optimizer was used with an initial learning rate (LR) of 0.0004. The training framework also utilized a scheduler to reduce LR by a factor of 10 every three epochs. The batch size was 400 and each training example had a duration of 3 s.

#### **4.4 Evaluation Metrics**

To evaluate different methods, we used PEAQ [24], PESQ [25] and SI-SDR [26] on the desired signal as the primary objective metrics. For a more detailed analysis of wind noise leakage, we employed the log-spectral distance (LSD) metric to compute the wind noise leakage metric  $\mathcal{L}$ , defined as follows:

$$\mathscr{L} \triangleq -\sqrt{\frac{1}{TF} \sum_{t=1}^{T} \sum_{f=1}^{F} \left( \log \left| \hat{D}_{t,f} \right| - \log \left| W_{t,f} \right| \right)^{2}}, \tag{11}$$

Table 1: Performance on the test set for scenarios with speech and instrumental music used as targets.

Processing	PLF	Params	RTF (%)	MHz	Speech			Ins. Music		
			<b>(, )</b>		PESQ	SI-SDR	Leakage $(\mathcal{L})$	PEAQ	SI-SDR	Leakage $(\mathcal{L})$
Noisy	-	-	-	-	1.80	3.03	-	-3.01	1.56	-
ULCNet	0.3	688K	0.127	182 MHz	2.23	12.75	-1.76	-	-	-
WindNet (Rej.)	0.3	365K	0.061	87 MHz	2.26	12.71	-2.72	-2.32	6.65	-2.90
WindNet (Ext.)	1.0	365K	0.061	87 MHz	2.26	13.90	-2.32	-2.59	7.58	-2.75
WindNetLite (Rej.)	0.3	249K	0.051	<b>73 MHz</b>	2.24	12.27	-2.81	-2.35	6.30	-2.80
WindNetLite (Ext.)	1.0	249K	0.051	<b>73 MHz</b>	2.23	14.31	-2.43	-2.57	7.67	-2.60

where  $\widehat{D}_{t,f}$  is the estimated desired signal complex STFT coefficient at time frame t and frequency bin f,  $W_{t,f}$  is the noise (wind) component coefficient, and T and F denote the total number of time frames and frequency bins, respectively. The negative sign before LSD is included to emphasize that a larger distance between the desired signal and noise corresponds to less leakage, indicating more effective wind noise reduction.

## 5 Results

## 5.1 Impact of Power-Law Factor

Our preliminary experiments have shown that the power-law compression described in Section 3 significantly affects performance. Although the power law factor  $\alpha=0.3$  was recommended in [13] for speech enhancement, this value may not be optimal for WNR depending on the target type, i.e., rejection or extraction. Thus, we evaluated WNR for  $\alpha$  from 0.3 to 1.0 in 0.1 increments for both modes. Figure 3 shows the wind noise leakage  $\mathscr L$  as a function of  $\alpha$ . For rejection,  $\alpha=0.3$  achieves the lowest leakage, whereas  $\alpha=1.0$  performs better for extraction. Informal listening tests confirmed these results, so we used  $\alpha=0.3$  for rejection and  $\alpha=1.0$  for extraction in all subsequent experiments.

## 5.2 Performance Comparison

Table 1 presents the WNR performance of our proposed WindNetLite and the baseline in both rejection and extraction modes, compared to the noisy signal. On the speech test set, WindNet achieves the highest PESQ score of 2.26, while WindNetLite matches ULCNet with a comparable score of 2.23. In terms of SI-SDR, extraction method outperform the rejection method, both WindNet and WindNetLite yield higher SI-SDR values (13.90 and 14.31), whereas in rejection mode they achieve lower leakage (-2.72 and -2.81). The ULCNet performs slightly lower than other models. However, it was trained for general speech enhancement rather than targeted WNR. On the instrumental music test set, rejection mode yields higher PEAQ scores (-2.32 for WindNet, -2.35 for Wind-NetLite). In extraction mode, WindNetLite slightly outperforms WindNet in SI-SDR, with scores of 7.67 dB and 7.58 dB, respectively. Leakage metrics show that rejection methods outperform extraction, with scores of -2.90 for WindNet and -2.80 for WindNetLite. In informal listening, we observe that the extraction mode introduces less distortion to the target signal, while the rejection mode provides stronger wind suppression. As a result,, the extraction method always achieves better SI-SDR results whereas the rejection method yields better leakage scores, since the leakage metric is more biased toward noise suppression.

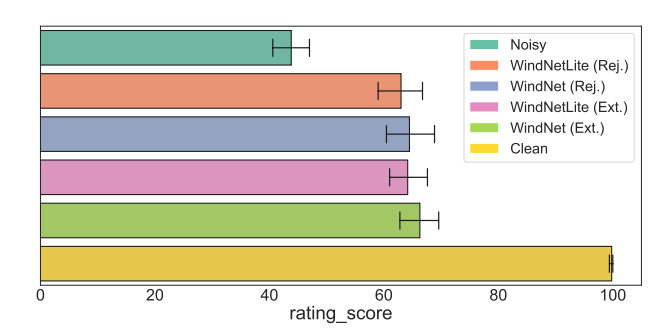


Figure 4: Results of MUSHRA listening test

In terms of computational complexity, both *WindNet* and *WindNetLite* significantly reduce computational costs compared to ULCNet, as evident from their parameter count and real-time factors (RTFs) measured on a single-core Cortex A53 1.43 GHz. As reported in Table 1, *Wind-Net* achieves an RTF of 0.061 (87 MHz), and *WindNetLite* reaches 0.051 (73 MHz).

#### **5.3 Subjective Evaluation**

To assess the subjective performance differences, we conducted a MUSHRA listening test. The test is carried out using the WebMUSHRA[27] framework, and the listeners were asked to rate the overall performance based on the signal quality and introduced distortions. In total, 10 listeners took part in the listening test, which consisted of 10 samples with signal-to-noise ratios ranging from -8 to -20 dB. The listeners were asked to rate the clean signal as 100, which was provided as the reference. As illustrated in Fig. 4, *WindNet* in extraction mode attained the highest mean rating of 66.29 while the other three models achieved comparable results. The listening samples can be found at https://fhgwnr.github.io/AIWNR/.

## 6 Conclusions

We have shown that leveraging wind noise spectral characteristics enables designing a very low-complexity DNN model suitable for resource-constrained embedded devices. Our proposed *WindNetLite* model requires only 40% of the RTF of the SOTA ULCNet and 84% of the baseline *WindNet* model, while achieving comparable results. We also show that it is important to study different hyperparameters and signal reconstruction methods to achieve a better trade-off between signal distortion and suppression quality.

## References

- [1] E. Nemer and W. Leblanc, "Single-microphone wind noise reduction by adaptive postfiltering," in *Proc. IEEE Workshop on Applications of Signal Processing to Audio and Acoustics (WASPAA)*, pp. 177–180, 2009.
- [2] C. M. Nelke, N. Nawroth, M. Jeub, C. Beaugeant, and P. Vary, "Single microphone wind noise reduction using techniques of artificial bandwidth extension," in *Proc. Euro*pean Signal Processing Conf. (EUSIPCO), pp. 2328–2332, 2012.
- [3] C. M. Nelke, P. A. Naylor, and P. Vary, "Corpus based reconstruction of speech degraded by wind noise," in *Proc. European Signal Processing Conf. (EUSIPCO)*, pp. 864– 868, 2015.
- [4] C. M. Nelke, N. Chatlani, C. Beaugeant, and P. Vary, "Single microphone wind noise PSD estimation using signal centroids," in *Proc. IEEE Intl. Conf. on Acoustics, Speech and Signal Processing (ICASSP)*, pp. 7063–7067, 2014.
- [5] J. Lee, K. Kim, T. Shabestary, and H.-G. Kang, "Deep bi-directional long short-term memory based speech enhancement for wind noise reduction," in *Proc. Hands-free Speech Communications and Microphone Arrays* (HSCMA), pp. 41–45, 2017.
- [6] H. Bai, F. Ge, and Y. Yan, "DNN-based speech enhancement using soft audible noise masking for wind noise reduction," *China Communications*, vol. 15, no. 9, pp. 235–243, 2018
- [7] G. W. Lee, K. M. Jeon, and H. K. Kim, "U-Net-based single-channel wind noise reduction in outdoor environments," in *Proc. IEEE Intl. Conf. on Consumer Electronics* (ICCE), pp. 1–2, 2020.
- [8] K.-Y. Lin, F.-M. Lai, and H.-Y. Chang, "Wind noise reduction strategy in hearing aids through U-Net deep learning and microphone enclosure design," *IEEE Sensors Journal*, vol. 24, no. 11, pp. 18307–18316, 2024.
- [9] S. Franz and J. Bitzer, "Multi-channel algorithms for wind noise reduction and signal compensation in binaural hearing aids," in *Proc. Intl. Workshop Acoust. Signal Enhancement* (IWAENC), 2010.
- [10] P. Thuene and G. Enzner, "Maximum-likelihood approach to adaptive multichannel-wiener postfiltering for wind-noise reduction," in *ITG Symp. on Speech Communication*, pp. 1–5, 2016.
- [11] D. Mirabilii and E. A. P. Habets, "Spatial coherence-aware multi-channel wind noise reduction," *IEEE/ACM Trans. Audio, Speech, Lang. Process.*, vol. 28, pp. 1974–1987, 2020.
- [12] O. Ronneberger, P. Fischer, and T. Brox, ""U-Net: Convolutional Networks for Biomedical Image Segmentation"," in *Medical Image Computing and Computer-Assisted Intervention MICCAI*, (Cham), pp. 234–241, Springer International Publishing, 2015.
- [13] S. S. Shetu, S. Chakrabarty, O. Thiergart, and E. Mabande, "Ultra low complexity deep learning based noise suppression," in *Proc. IEEE Intl. Conf. on Acoustics, Speech and Signal Processing (ICASSP)*, Apr. 2024.
- [14] S. S. Shetu, E. A. Habets, and A. Brendel, "Comparative Analysis of Discriminative Deep Learning-Based Noise Reduction Methods in Low SNR Scenarios," in *Proc. Intl.* Workshop Acoust. Signal Enhancement (IWAENC), 2024.
- [15] C. Zheng, H. Zhang, W. Liu, X. Luo, A. Li, X. Li, and B. C.

- Moore, "Sixty years of frequency-domain monaural speech enhancement: From traditional to deep learning methods," *Trends in Hearing*, vol. 27, 2023.
- [16] X. Hao, X. Su, S. Wen, Z. Wang, Y. Pan, F. Bao, and W. Chen, "Masking and inpainting: A two-stage speech enhancement approach for low SNR and non-stationary noise," *IEEE International Conference on Acoustics, Speech and Signal Processing (ICASSP)*, pp. 6959–6963, 2020.
- [17] S. Kuroiwa, Y. Mori, S. Tsuge, M. Takashina, and F. Ren, "Wind noise reduction method for speech recording using multiple noise templates and observed spectrum fine structure," in 2006 International Conference on Communication Technology, pp. 1–5, 2006.
- [18] S. S. Shetu, N. K. Desiraju, J. M. M. Aponte, E. A. Habets, and E. Mabande, "A hybrid approach for low-complexity joint acoustic echo and noise reduction," in *Proc. Intl. Work-shop Acoust. Signal Enhancement (IWAENC)*, 2024.
- [19] S. S. Shetu, N. K. Desiraju, W. Mack, and E. A. Habets, "Align-ULCNet: Towards Low-Complexity and Robust Acoustic Echo and Noise Reduction," arXiv preprint arXiv:2410.13620, 2024.
- [20] N. K. Rao, S. R. Chetupalli, S. S. Shetu, E. A. Habets, and O. Thiergart, "Low-complexity neural speech dereverberation with adaptive target control," in *ICASSP 2025-2025 IEEE International Conference on Acoustics, Speech and Signal Processing (ICASSP)*, pp. 1–5, IEEE, 2025.
- [21] J. F. Gemmeke, D. P. Ellis, D. Freedman, A. Jansen, W. Lawrence, R. C. Moore, M. Plakal, and M. Ritter, "Audio set: An ontology and human-labeled dataset for audio events," in 2017 IEEE international conference on acoustics, speech and signal processing (ICASSP), pp. 776–780, IEEE, 2017.
- [22] J. Yamagishi, C. Veaux, and K. MacDonald, "CSTR VCTK Corpus: English Multi-speaker Corpus for CSTR Voice Cloning Toolkit (version 0.92), [sound].," University of Edinburgh. The Centre for Speech Technology Research (CSTR), 2019.
- [23] Z. Rafii, A. Liutkus, F.-R. Stöter, S. I. Mimilakis, and R. Bittner, "The MUSDB18 corpus for music separation," Dec. 2017.
- [24] T. Thiede, W. C. Treurniet, R. Bitto, C. Schmidmer, T. Sporer, J. G. Beerends, and C. Colomes, "PEAQ-The ITU standard for objective measurement of perceived audio quality," *Journal Audio Eng. Soc.*, vol. 48, no. 1/2, pp. 3–29, 2000.
- [25] A. W. Rix, J. G. Beerends, M. P. Hollier, and A. P. Hekstra, "Perceptual evaluation of speech quality (PESQ)-a new method for speech quality assessment of telephone networks and codecs," *IEEE international conference on acoustics, speech, and signal processing. Proceedings (ICASSP)*, vol. 2, pp. 749–752, 2001.
- [26] J. Le Roux, S. Wisdom, H. Erdogan, and J. R. Hershey, "SDR-half-baked or well done?," in *Proc. IEEE Intl. Conf.* on Acoustics, Speech and Signal Processing (ICASSP), pp. 626–630, 2019.
- [27] M. Schoeffler, F.-R. Stöter, B. Edler, and J. Herre, "Towards the next generation of web-based experiments: A case study assessing basic audio quality following the itu-r recommendation bs. 1534 (mushra)," in *1st Web Audio Conference*, pp. 1–6, 2015.